Structure of the superconducting $La_2CuO_{4+\delta}$ phases ($\delta \approx 0.08, 0.12$) prepared by electrochemical oxidation

P. G. Radaelli
Science and Technology Center for Superconductivity, Argonne National Laboratory, Argonne, Illinois 60439

J. D. Jorgensen
Materials Science Division, Argonne National Laboratory, Argonne, Illinois 60439

A. J. Schultz
Chemistry and Materials Science Divisions, Argonne National Laboratory, Argonne, Illinois 60439

B. A. Hunter and J. L. Wagner
Science and Technology Center for Superconductivity, Argonne National Laboratory, Argonne, Illinois 60439

F. C. Chou and D. C. Johnston
Ames Laboratory and Department of Physics and Astronomy, Iowa State University, Ames, Iowa 50011
(Received 19 February 1993)

Two powder samples of electrochemically oxidized $La_2CuO_{4+\delta}$ (nominally $\delta \approx 0.08$ and 0.12) and one single crystal ($\delta \approx 0.1$), with superconducting critical temperatures of 32, 42, and 40 K, respectively, were studied using neutron diffraction. All samples appear to be single phase, both at room temperature and at low temperature (10–18 K), as evidenced by sharp Bragg peaks, indicating that these samples have compositions beyond the phase-separated region of the phase diagram. A detailed analysis of the Bragg reflections demonstrated that the basic crystallographic structure of all samples has *Fmmm* symmetry, with the excess oxygen located between adjacent LaO layers. However, a number of low-intensity peaks in the powder data suggested the existence of a very large superstructure. The satellites could be clearly identified in the single-crystal data, allowing the propagation vectors of the modulation to be determined. Rietveld refinements of the average structure, based on the main Bragg peaks, are presented here for samples prepared with this technique.

I. INTRODUCTION

The family of cuprate superconductors based on the K_2NiF_4 structure, hereafter referred to as the "2:1:4" structure, has been the subject of an extraordinary research effort in recent years. The hope has been that intensive study of this relatively simple structure could shed light on a series of phenomena that are presumed to be common to a larger class of compounds. The correlations between crystal structure, electronic doping, and superconducting properties are among the most important issues to be addressed.

La_2CuO_4 is the best known cuprate having the 2:1:4 structure. The stoichiometric compound is an antiferromagnetic insulator, but can be doped to produce a superconductor, with a maximum T_c as high as 40 K, by partially replacing La with an alkaline earth or an alkali metal (Ba, Sr, Ca, Na, K,. . .)[1–4] or by introducing interstitial oxygen into the structure.[5–7] The latter is usually accomplished by annealing the samples at high temperature (~500 °C) in a high oxygen partial pressure.[8,9] Because of a miscibility gap in the phase diagram, pressures around 25 kbar are required to obtain single-phase superconducting samples.[10,11] The amount of interstitial oxygen has been a subject of controversy, the measured value being strongly dependent on the measurement technique. Thermogravimetric analysis (TGA) often yields higher values of δ than does iodometric titration.[12] The observation of O_2^- species by x-ray photoemission spectroscopy[12,13] initially suggested that interstitial oxygen atoms may form a superoxide species in the lattice. Later, the presence of a large amount of superficial oxygen was proposed as an alternative explanation.[10] Heat capacity measurements on a polycrystalline sample, prepared at 600 °C under 3 kbar O_2, have shown that, at least for some synthesis schemes, a large fraction of the excess oxygen is molecular O_2, presumably on the surface and in microvoids of the sample.[14] Such measurements have all supported the conclusion that superficial oxygen, not in the $La_2CuO_{4+\delta}$ crystal lattice, is responsible for the discrepancies. As we will later discuss, a similar discrepancy between TGA and iodometric titration results is also found for electrochemically oxidized samples. However, we will present a hypothesis for explaining this discrepancy that does not require the presence of superficial oxygen.

Jorgensen and co-workers studied several powder samples of $La_2CuO_{4+\delta}$, prepared at intermediate pressures and temperatures [$p(O_2) \leq 3$ kbar, $T \sim 500$ °C], by neutron powder diffraction,[15] and concluded that the superconducting compound resulted from phase separation near room temperature into two quasi-isostructural phases.

The amount of superconducting phase was found to increase linearly with the total oxygen content of the samples. This fact, along with the observation that the structural parameters of the second (nonsuperconducting) phase closely matched those of the stoichiometric La_2CuO_4 compound, allowed the oxygen content of the superconducting phase to be estimated at $\delta \approx 0.08$, based on the "lever rule" and the assumption that the antiferromagnetic insulating phase had $\delta = 0$. Both the insulating and the superconducting phase were found to have orthorhombic symmetry.[16,17]

The small amount of interstitial oxygen and the presence of phase separation in $La_2CuO_{4+\delta}$ samples prepared under intermediate conditions has been a serious obstacle to the determination of the exact crystal structure of the superconducting compound and the location of the interstitial oxygen atoms. Samples annealed under higher pressures ($\sim$25 kbar) contained only one 2:1:4 phase,[10,11] but their relatively poor quality (broad diffraction peaks, presence of nonisostructural impurity phases) made them unsuitable for definitive crystallographic studies.

For this reason, the isostructural compound $La_2NiO_{4+\delta}$ was studied. $La_2NiO_{4+\delta}$ displays a miscibility gap similar to the cuprate compound, which suggests that the structure of the oxygen defect might be the same for both systems. High-quality samples of $La_2NiO_{4+\delta}$, with excess oxygen concentrations of $\delta \approx 0.2$, well beyond the well-known miscibility gap, can be easily synthesized.[18] Jorgensen and co-workers succeeded in determining the defect structure of $La_2NiO_{4.18}$ from neutron powder diffraction data.[19] The interstitial oxygen was found to be located between the two LaO layers, and to be tetrahedrally coordinated to four La atoms. For this compound, the amount of excess oxygen indicated by TGA measurements in H_2 agreed perfectly with the amount of interstitial oxygen located by neutron powder diffraction. Some features of the structural distortion around the interstitial could also be determined from this analysis. Based on the analysis of systematic absences, the structure of the oxygen-rich phase was concluded to have a higher symmetry (*Fmmm*) than the stoichiometric compound (*Bmab*). It was speculated that the higher symmetry resulted from frustration of the *Bmab* tilting pattern by the interstitial oxygen.

In 1989 Chaillout and co-workers published the result of a neutron-diffraction study on a $La_2CuO_{4.032}$ single crystal.[20] Their work confirmed that the defect structure model proposed by Jorgensen for $La_2NiO_{4+\delta}$ was also applicable to the cuprate system, at least in its general features. The single-crystal data presented in their work were obtained in a region of the phase diagram where $La_2CuO_{4+\delta}$ is known to have a miscibility gap. In an attempt to address this problem, Chaillout and co-workers presented further refinements of single-crystal neutron-diffraction data based on a two-phase model.[21] A detailed analysis of the peak profiles of low-symmetry reflections that are allowed by the *Bmab* space group but forbidden in *Fmmm*, led the authors to assign the former space group to the superconducting structure as well. As a consequence, they proposed a modified version of the structural distortion around the interstitial, that included a short O-O bond.

The development of room-temperature chemical[22] and electrochemical[23–25] techniques suitable for inserting oxygen into the 2:1:4 oxides has recently allowed the room-temperature synthesis of $La_2CuO_{4+\delta}$, $La_{2-x}Sr_xCuO_{4+\delta}$, and $La_2NiO_{4+\delta}$ samples with very high values of δ. This is particularly significant in the case of the cuprate system, making high-quality, single-phase superconducting samples of $La_2CuO_{4+\delta}$ available.

Detailed measurements of the magnetic and transport properties of electrochemically oxidized $La_2CuO_{4+\delta}$ have been reported.[24–26] Only superconducting transitions at 32 and 42–45 K were observed in these studies, the lower T_c being found in samples with lower oxygen content. This observation suggested that two chemically and/or structurally distinct phases may be present at low temperature. Grenier and co-workers studied the phase diagram of $La_2CuO_{4+\delta}$ by x-ray, electron and neutron powder diffraction.[24,25]. These authors used iodometric titration to determine the oxygen content of their samples. As we have already mentioned, iodometric titration and TGA often yield quite different values of the oxygen content for these materials. We will later discuss some of the possible interpretations of this disagreement. In order to avoid confusion, we prefer to describe iodometric titration results in terms of the formal copper oxidation state $(2+P)$ rather than δ. P is sometimes referred to as "hole concentration," although this definition has to be taken with some caution. Grenier and co-workers calculate δ for their samples, that cover the range $0 \le P \le 0.18$, using the formula $\delta = P/2$. The structural analysis confirmed some of the features already established for the $La_2NiO_{4+\delta}$ system, such as the presence of a miscibility gap, and suggested the existence of a series of modulated structures. Particularly interesting is the fact that the room-temperature a, b, and c lattice parameters display a sharp discontinuity in the first derivative for $P \approx 0.10$. The orthorhombic strain has a pronounced minimum for $P \approx 0.10$, its value for $P \approx 0.18$ being larger than that of the $P = 0.00$ sample. Previous data on the $La_2NiO_{4+\delta}$ system also showed the presence of a minimum in the orthorhombic strain,[19] although the absolute maximum of the orthorhombic strain occurred for the stoichiometric ($\delta = 0.00$) sample. Grenier and co-workers suggested that the discontinuity in the structural parameters may be associated with a change in the ordering of the interstitial oxygen defects. However, no structural parameters other than the lattice constants have been reported to support this hypothesis.

In this paper, we present structural refinements of Neutron-diffraction data from two powder samples ($\delta = 0.08$, with $T_c \approx 32$ K, and 0.12, with $T_c \approx 42$ K) of superconducting $La_2CuO_{4+\delta}$, and of neutron-diffraction data from a superconducting $La_2CuO_{4+\delta}$ ($\delta \approx 0.1$) single crystal obtained by electrochemical oxidation.

II. SAMPLE PREPARATION AND CHARACTERIZATION

The details of preparation of polycrystalline $La_2CuO_{4+\delta}$ are described elsewhere.[26] The electrochemi-

cal cell is set up as

$$La_2CuO_4/1\ N\ NaOH/Pt\ ,$$

where the working electrode is a pellet or a single crystal of La_2CuO_4 and the counter electrode is a platinum wire. Two powder samples with different oxygen contents were prepared.

The powder sample with higher oxygen content was made from ~ 3.8 g of La_2CuO_4 powder, which was compressed together with a thin platinum wire into a cylindrical shape. The platinum wire embedded in the sample electrode was used for electrical contact. A constant anodic current of 1 mA was passed through the sample electrode until a total charge $Q = 0.32$ electron/formula unit (e/f.u.) was reached. The final product was ground, washed with distilled water and absolute alcohol several times, then dried in vacuum ($\sim 10^{-3}$ Torr) at room temperature for more than 9 h.

The powder sample with lower oxygen content was prepared using a slightly different technique. Two annealed thin pellets (~ 3 g each) with diameter 2.54 cm and thickness ~ 0.2 mm were used as working electrodes. Electrical contact was made using a platinum wire attached with silver paint. The silver paint was covered with silicone rubber. A constant potential of 0.6 V (relative to a Ag/AgCl reference electrode) was applied to the sample electrode for 6 days without stirring the electrolyte. The open circuit potential approaches, but does not reach, 0.4 V after this treatment. Previous work has indicated that the open circuit potential versus charge-transfer curve displays a plateau at 0.4 V for $Q \geq 0.16$ e/f.u.[26] Therefore, we conclude that $Q \leq 0.16$ e/f.u. An additional charge $Q \sim 0.15$ e/f.u. was passed through the cell at constant currents of 1 mA for 2 days and 100 μA for 3.5 days. The final product was washed and dried following the same procedure as described above.

A single crystal of La_2CuO_4 of mass 36.35 mg and dimensions $4.5 \times 2 \times 1$ mm^3 was grown using a flux method.[27] A platinum wire was attached to one side of the crystal using silver paint. The silver paint was fully covered with silicone rubber. An anodic current of 100 μA was applied to the cell, yielding $Q \sim 0.33$ e/f.u. A superconducting phase is expected at this value of Q for polycrystalline samples,[26] but no superconductivity was observed for the crystal above 6 K, using dc magnetization. Additional oxidation at a current of 100 μA for 4 days ($Q \sim 4$ e/f.u.) led to only traces of superconductivity. Bulk superconductivity and homogeneous oxidation were achieved (see below) after additional charging with a 10 μA current for more than a month. For the present powder and single-crystal samples, the integrated current Q cannot be used to estimate the value of δ, because of possible oxygen evolution in gaseous form.

The oxygen contents of the $La_2CuO_{4+\delta}$ powder samples were measured using TGA analysis. About 20 mg of powder was heated under 1 atm of He gas, and the value of δ was determined from the weight loss between ~ 180 and ~ 380 °C (Ref. 26) as shown in Figs. 1(a) and 1(b). The excess oxygen content of the two powder samples were $\delta = 0.11 \pm 0.01$ and $\delta = 0.07 \pm 0.01$, respectively. The continuous weight loss below ~ 180 °C corresponds to about 0.01 oxygen atoms/f.u. which may be considered to be a lower limit to the amount of superficial (molecular) oxygen and/or equivalent residual electrolyte. The oxygen content was also determined using TGA in a H_2 atmosphere, as shown in Figs. 1(c) and 1(d). From the weight loss between room temperature and 760 °C, the excess oxygen contents of the two powder samples were found to be $\delta = 0.12 \pm 0.01$ and $\delta = 0.09 \pm 0.01$, respectively. The agreement, within the error bars, between the two techniques indicates that the presence of electrolyte trapped in the pores does not affect significantly the relia-

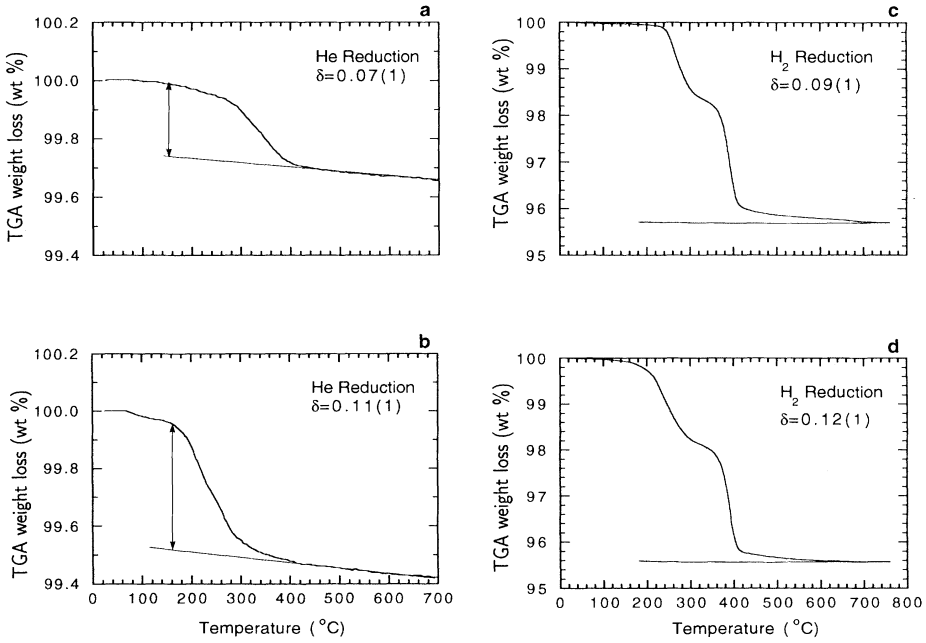

FIG. 1. TGA weight-loss curves for $La_2CuO_{4+\delta}$ powder samples, for $\delta \approx 0.08$ and $\delta \approx 0.12$, in 1 atm He gas (a and b) and in 1 atm H_2 gas (c and d). Upper and lower lines in c and d represent heating and cooling curves, respectively.

TABLE I. Comparisons of the oxygen contents determined by TGA in He, TGA in H_2 and iodometric titration for doped and undoped La_2CuO_4. Data in rows 1 and 2 are from the powder samples of the present work. Data in rows 3 and 4 are from Refs. 15 and 26, respectively. The datum in row 5 is from Ref. 26, and shows that iodometric titration correctly measured the expected hole concentration in Sr-doped La_2CuO_4. Columns 4 and 5 contain the values of δ as calculated from P, assuming the final state of the excess oxygen in the acidic solution used for titration to be O^{2-} and $(O_2)^{2-}$, respectively.

Samples	δ from TGA H_2 reduction	δ from TGA He reduction	P(e/f.u.) from titration	δ from P with O^{2-} assumed	δ from P with $(O_2)^{2-}$ assumed
$La_2CuO_{4+\delta}$	0.09(1)	0.07(1)	0.08(2)[a]	0.04	0.08
$La_2CuO_{4+\delta}$	0.12(1)	0.11(1)	0.14(2)[a]	0.07	0.14
La_2CuO_4[b]		0.00(1)			
La_2CuO_4[c]	0.02(1)		0.00(2)	0.00	0.00
$La_{1.85}Sr_{0.15}CuO_4$[c]			0.14(2)		

[a]Average of three measurements.
[b]From Ref. 15.
[c]From Ref. 26.

bility of the TGA measurements, since the weight loss due to the evaporation of the electrolyte is expected to occur for $T < 180\,^{\circ}C$.

Iodometric titration performed on the same samples yielded $P = 0.08 \pm 0.02$ and $P = 0.14 \pm 0.02$, respectively. The values of δ from TGA (in He and H_2) and the value of P from iodometric titration are compared in Table I. For comparison, additional data for undoped La_2CuO_4 and for $La_{1.85}Sr_{0.15}CuO_4$, prepared with conventional techniques, are also listed. In the latter two cases iodometric titration yields the expected values within the error bars.

It is clear from these data that, for $La_2CuO_{4+\delta}$, the value of δ from TGA is much larger than $P/2$. This is consistent with previous literature data, (see Sec. I) and our previous results.[26] This discrepancy indicates that part of the weight loss during the TGA measurement is caused by a species that does not transform into O^{2-} upon dissolution in the acidic solution used for iodometric titration. Two possible explanations can be proposed. (i) There is a very large amount of superficial (molecular) oxygen in the samples, that is released only for $T > 180\,^{\circ}C$ in the TGA measurements. This species is liberated as gaseous or water-dissolved O_2 in the acidic solution. (ii) A significant amount of anionic bonding occurs between oxygen atoms in the material. Part or all of these covalently bonded oxygen atoms remain bonded in the solution, forming H_2O_2 or other peroxide species. We believe the second possibility to be more likely.

The need to use nondestructive techniques to measure δ for the single crystal makes it difficult to obtain a reliable and accurate value for the oxygen content. The

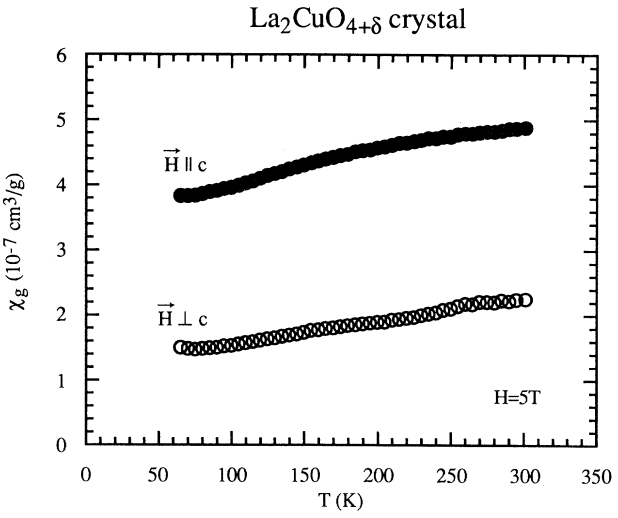

FIG. 2. Normal-state magnetic susceptibility as a function of temperature, for a single crystal of $La_2CuO_{4.1}$. The data were obtained using a SQUID magnetometer, with an applied magnetic field of 5 T. Open and closed circles represent data taken with the magnetic field perpendicular and parallel to the c axis, respectively.

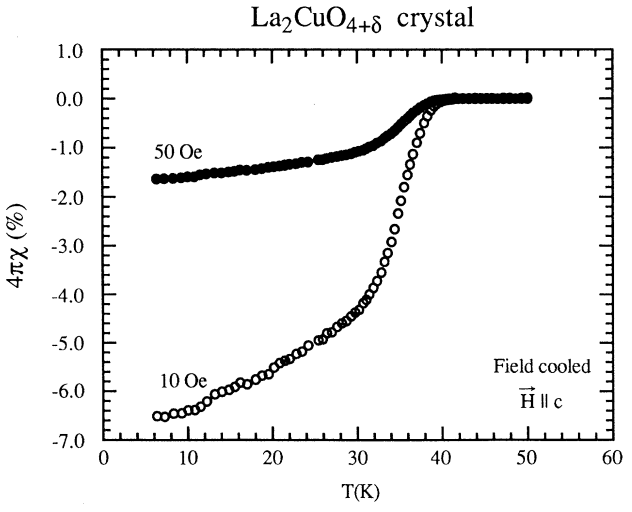

FIG. 3. Field-cooled dc magnetization measurements for a single crystal of $La_2CuO_{4.1}$, in an applied magnetic field of 10 Oe (open circles) and 50 Oe (closed circles). The data were obtained using a SQUID magnetometer.

measured 0.19 mg weight gain after oxidation yields $\delta=0.13\pm0.02$. On the other hand, the observation that T_c for the crystal is intermediate between those of our two powder samples, and that the orthorhombic strain at low temperature for the crystal is smaller than for the 0.12 powder sample, suggests a value of δ which is intermediate between those of the two powder samples.

Normal-state magnetic susceptibility $\chi(T)$ was measured for all samples in a 50 kOe applied field, using a SQUID magnetometer. An anomaly near 250 K would signal the presence of near stoichiometric La_2CuO_4,[28] resulting from phase separation or from nonoxidized starting material. The data for our samples show no evidence of such an anomaly, indicating that no antiferromagnetic phase is present at low temperature, and, thus, the value of δ lies beyond the miscibility gap. Normal-state dc susceptibility data for the single crystal are shown in Fig. 2. The temperature dependence and anisotropy are similar to those of optimally doped $La_{2-x}Sr_xCuO_4$.[28]

Field-cooled (FC) and zero-field-cooled (ZFC) dc magnetization measurements in low fields (10 and 50 Oe) were used to determine the superconducting properties. The onset critical temperatures T_c for the two polycrystalline samples with $\delta=0.12$ and $\delta\approx0.08$ were 42 and 32 K, respectively. Superconducting phase fractions at 6 K in a magnetic field of 10 Oe, calculated with no demagnetization factor correction, were 26% (FC) and 33% (ZFC) for the sample with $T_c=42$ K, and 24% (FC) and 26% (ZFC) for the sample with $T_c=32$ K.

The onset T_c for the single-crystal sample is ~40 K. In Fig. 3, dc susceptibility FC curves for a field perpendicular to the CuO_2 layers are shown. The Meissner fraction, measured in a 10 Oe field at 6 K, with no correction for demagnetization effects, is 6% of the maximum theoretical value, whereas the shielding fraction (not shown) is 210% at the same temperature and magnetic field. These data suggest that flux-pinning effects may be strong.

III. NEUTRON-DIFFRACTION DATA ACQUISITION AND ANALYSIS

Neutron powder diffraction data were collected on the two powder samples, at room temperature and 10 K, using the special environment powder diffractometer (SEPD) at the Argonne intense pulsed neutron source (IPNS).[29] For the low-temperature data collection, the instrument was equipped with a closed-cycle helium refrigerator (Displex), with an average cooling rate of 3–5 K/min. The samples were contained in vanadium tubes sealed under a helium atmosphere. For comparison, a sample of stoichiometric La_2CuO_4 was run under identical conditions.

The powder diffraction data were analyzed with the Rietveld technique, using the IPNS code.[30,31] Only data from the high-resolution backscattering detector banks ($2\theta=145°$) were used in the refinements. Bragg peaks from both powder samples displayed a small and temperature-independent width. The σ_1 parameter that accounts for instrumental and strain broadening effects, was refined to a value comparable to the instrumental resolution for the $\delta=0.08$ sample, and to a value only slightly higher for the $\delta=0.12$ sample. In contrast to the results previously obtained for samples with lower oxygen content,[15] no anomaly in the line shapes that would suggest the coexistence of two phases is present for either sample, at room temperature or at 10 K. We thus concluded that both powder samples were nominally single phase.

Single-crystal neutron-diffraction data were collected at 18 K, using the time-of-flight single-crystal diffractometer (SCD) at IPNS, equipped with a large area (30×30 cm^2) position sensitive detector and a closed-cycle refrigerator.[32] The crystal was mounted at the end of an aluminum pin using low-temperature adhesive, and cooled at an average rate of 3 K/min. With a stationary crystal and detector, a three-dimensional histogram of a portion of reciprocal space was obtained. For this study, 16 histograms were collected, with the crystal in different orientations, so that more than an octant of reciprocal space was covered. Integrated intensities of Bragg reflections were obtained using the IPNS-SCD single-crystal analysis package.[33] Structure refinement was performed using a multiwavelength program [Argonne National Lab Variable Wavelength Least-Square program (ANVLS)] based on the Oak Ridge Fortran Least-Square program (ORFLS).[34]

High-q reflections from the single-crystal data set are split, indicating the presence of twinning. It is highly probable that the crystal was already twinned before oxygen intercalation, since it was cooled through the tetragonal to orthorhombic phase transition after the growth process. A close analysis of the profiles of the $[h,\bar{h},l]$ Bragg peaks (Fig. 4) indicates that only two sets of domains, related by a mirror reflection through the

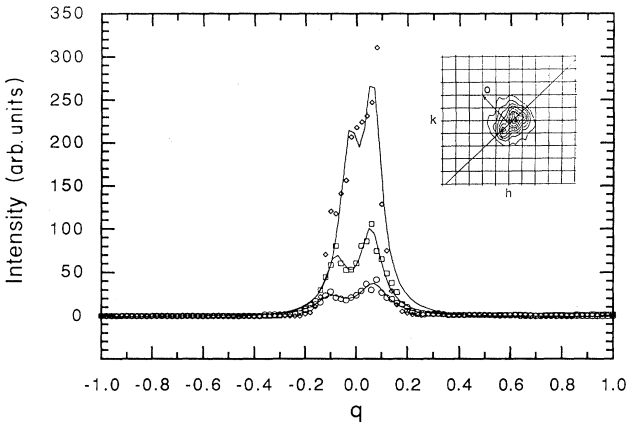

FIG. 4. Reciprocal space intensity profiles through the Bragg reflections $[10,\bar{1}0,0]$ (circles), $[8,\bar{8},0]$ (squares), and $[6,\bar{6},0]$ (diamonds), obtained from single-crystal neutron-diffraction data at 18 K. The splitting of the reflections is due to twinning. Profiles are taken along the reciprocal space lines $[h+q,-h+q,0](h=6,8,10)$, parallel to the [1,1,0] direction, as indicated in the inset, and are plotted as a function of the linear parameter q. The arrow in the inset indicates the direction to the origin. The data are fit with the sum of two Lorentzian functions with identical full width at half maximums (FWHM) (solid lines).

$[h,h,l]$ plane, are present, and that the relative proportion of the two individuals is approximately 37:63%. Using this information, the intensities due to each individual can be deconvoluted, without the need to resolve all Bragg reflections. However, in order to preserve the original statistics, we preferred an alternative approach: using an *ad hoc* modified version of the ANVLS code, a twinning operation is applied to the calculated intensities before they are compared with the observed intensities. The percentage of the two individuals can either be fixed to the previously obtained value, or refined along with the other parameters. Both methods yield very similar values for the structural parameters. The value of the orthorhombic strain can be calculated using the split reflections.

IV. SPACE-GROUP SYMMETRY: CONVENTIONS

For the sake of simplicity we prefer to use a consistent set of axes to describe the various structural modifications. According to our convention, the c axis is taken as the longest one. The a axis is the "tilt" axis, that is, the axis of rotation of the CuO_6 octahedra, in the stoichiometric La_2CuO_4. As a consequence, the O2 (apical oxygen atoms) and La atoms have a nonzero y coordinate, while the O1 (planar oxygen atoms) have a nonzero z coordinate. In the $La_2CuO_{4+\delta}$ samples, there is no coordinated tilt pattern, at least within the fundamental cell. However, all attempted refinement models agree in indicating that part or all of the apical O2 oxygen atoms

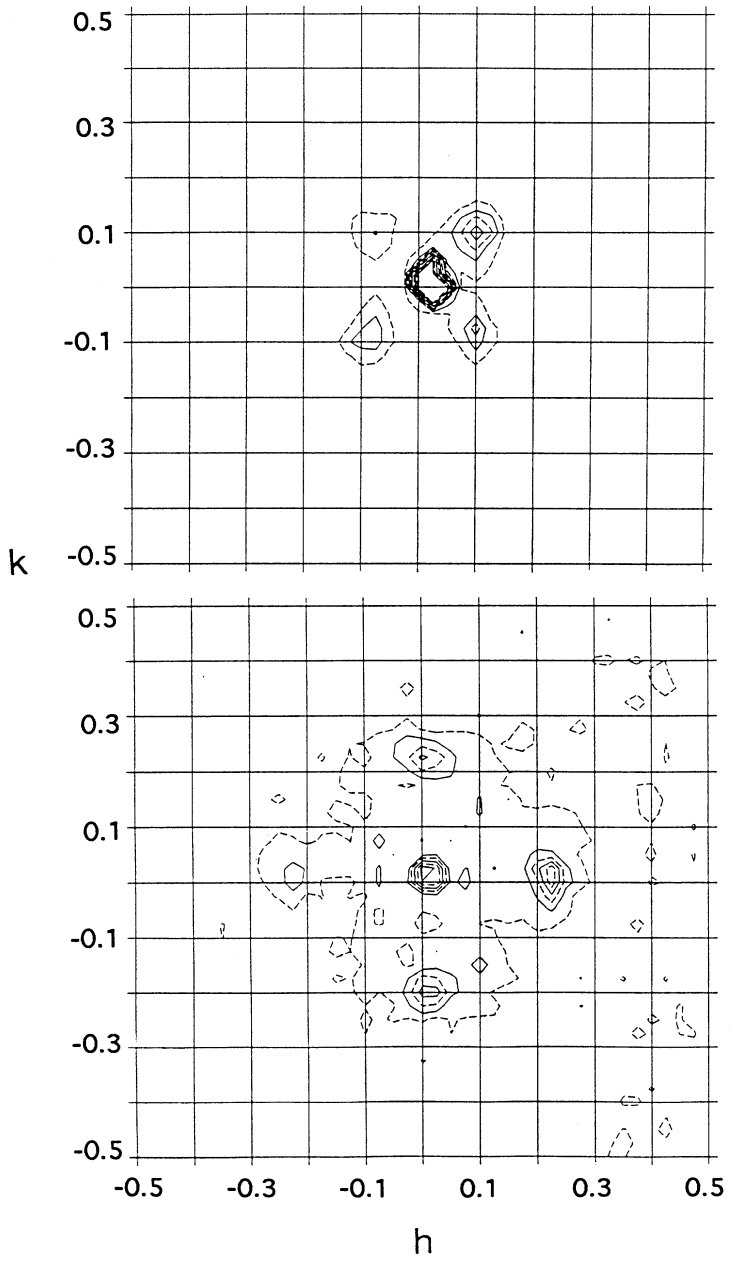

FIG. 5. Intensity contour plots of reciprocal space sections perpendicular to the c^* direction, at (a) $l=5.83$ and (b) $l=5.67$. Satellites with propagation vectors (a) $(\pm 0.1, \pm 0.1, -0.167)$ and (b) $(0, \pm 0.2, -0.333)$ or $(\pm 0.2, 0, -0.333)$ appear around the tail of the [0,0,6] Bragg reflection.

are displaced off the high-symmetry position. Therefore, the *b* axis is chosen to be parallel to the largest component of these displacements. In all the cases we examined, the *a* axis turned out to be the shortest one.

V. LATTICE SYMMETRY

The stoichiometric compound La_2CuO_4 has space-group symmetry *Bmab*. This structure can be understood in simple terms as derived from the *I4/mmm* (HTT) structure by quasirigid tilts of the CuO_6 octahedra around the tetragonal [110] axis. Adjacent octahedra are rotated in opposite directions, giving rise to a characteristic wavelike corrugation pattern of the CuO_2 planes and to a doubling of the volume of the original unit cell. The corrugation patterns of two CuO_2 planes in the same unit cell are related by a [1/2, 0, 1/2] translation (*B* centering). Diffraction patterns from the *Bmab* structure are characterized by the presence of small peaks that are extinct both in the *I4/mmm* and in the *Fmmm* structures. These *Bmab* peaks are not observed in the $\delta \approx 0.08$ or $\delta \approx 0.12$ powder data. The single-crystal data also confirm the absence of such peaks. We will discuss later the presence of additional weak reflections off the main reciprocal lattice that implies the existence of a large supercell. However, the extinction rules for the reflections on the reciprocal lattice generated by the fundamental ($\sim 5.4 \times 5.4 \times 13.2$) cell are consistent with the *Fmmm* space group. We conclude, therefore, that the space group of the structure under investigation, averaged through all $\sim 5.4 \times 5.4 \times 13.2$ lattice translations, is *Fmmm*.

VI. SUPERSTRUCTURE

The diffraction patterns of both powder samples show evidence of broad low-intensity peaks that cannot be indexed either with the original cell or with any simple superstructure. Single-crystal analysis shows the presence of satellites around several Bragg peaks, as well as around forbidden peaks. Figures 5(a) and 5(b) show contour plots of two sections of reciprocal space in the vicinity of the [0,0,6] Bragg reflection, at $l = 5.83$ and 5.67, respectively. In Fig. 6, a large section of reciprocal space is represented in a schematic way. The reciprocal lattice defined by the satellites appears to be commensurate with the original one: all observed reflections can be indexed using an *F* centered $10a \times 10b \times 6c$ supercell. However, the observed satellite pattern could result from the superposition of more than one set of superlattice reflections, each with a smaller supercell. Electron-diffraction analysis for similar samples[24] has evidenced the simultaneous presence of more than one set of superlattice reflections on powder samples that appear to be single phase, as far as the main reflections are concerned.

Figure 7 shows a line in reciprocal space parallel to c^*, passing through the $[0,\bar{5},2]$ reciprocal-lattice point. The two superlattice reflections at $l = 2 \pm 1/3$ are clearly identifiable. We note that, due to intrinsic linewidth and to poor instrumental resolution, some intensity is observable also at the $[0,\bar{5},2]$ position, which would correspond to a *Bmab*-allowed reflection. The appearance of satellites around forbidden reflections indicates that the distortion associated with the modulation locally breaks the *Fmmm* symmetry. Modulated structures are commonly observed in the isostructural compound $La_2NiO_{4+\delta}$.[35,36]

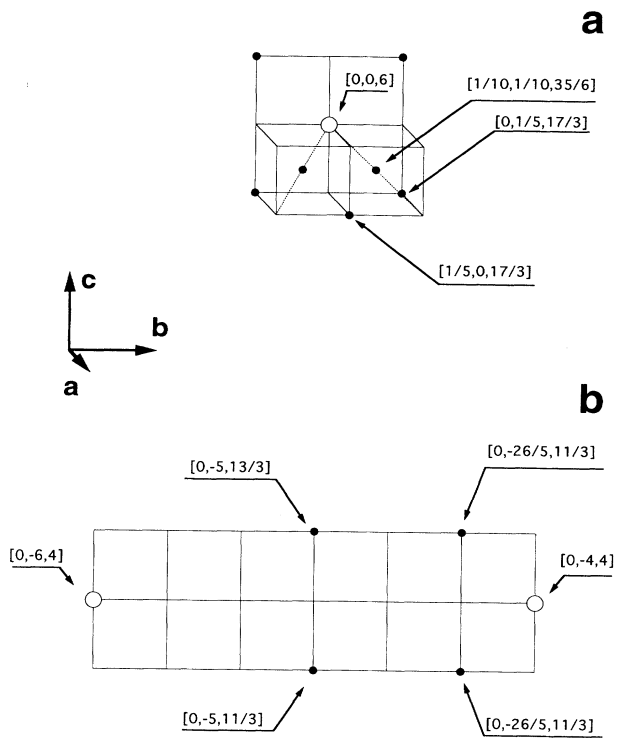

FIG. 6. Schematic representation of the reciprocal space around the [0,0,6] Bragg reflection (a) and the $[0,\bar{5},4]$ "forbidden" position (b), from single-crystal neutron-diffraction data. Open and closed circles represent fundamental and superlattice reflections, respectively.

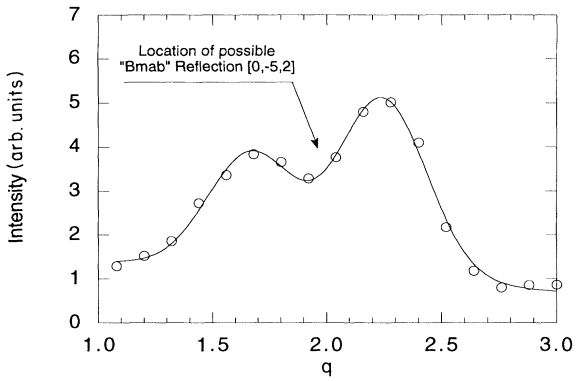

FIG. 7. Reciprocal space intensity profile through the $[0,\bar{5},2]$ reciprocal lattice point, from single-crystal neutron-diffraction data (open circles). The profile is taken along the reciprocal space line $[0,\bar{5},q]$, parallel to the c^* direction, and is plotted as a function of the linear parameter *q*. The data are fit with the sum of two Gaussian functions with identical FWHM (solid line). The arrow indicates the position of a possible *Bmab* reflection.

VII. STRUCTURAL REFINEMENT FOR SINGLE-CRYSTAL DATA

A refinement of structural parameters was carried out in the *Fmmm* space group, using single-crystal data collected at low temperature. Only reflections consistent with the $\sim 5.4 \times 5.4 \times 13.2$ unit cell were considered. Integrated intensities were corrected for the wavelength-dependent incident flux, detector efficiency, and absorption using a spherical model. A twinning operation was applied to the calculated structure factors before comparing them with the observed ones, as explained above. The domain volume ratio was set at the value obtained from the analysis of the $[h,\bar{h},l]$ reflections (37:63%). This procedure forced us to minimize the value of χ^2 based on F^2's, rather than on F's, since the square root of the observed intensities no longer has the meaning of the modulus of the structure factor. The full data set consisted of 16 separate histograms, with partial overlapping. The scale factors of each histogram, as well as an overall isotropic extinction parameter, were included among the refined parameters.

A preliminary set of refinements, in which all atoms were constrained to high-symmetry positions, led to a deficient value for the occupancy of the O2 (apical) site. Therefore, following the scheme proposed by Jorgensen and co-workers for the $La_2NiO_{4+\delta}$ system,[19] a displaced apical site O4 was added, in a general $h32(x,y,z)$ position. We assume that the displacement of part of the apical oxygen atoms to the O4 site results from the insertion of the interstitial oxygen defect (O3). The three coordinates of O4 were refined, starting in the vicinity of the O2 position. If the remaining O2 atoms are left in high-symmetry positions, their thermal ellipsoids displayed anisotropic as well as anharmonic character. Therefore, the O2 atoms were also allowed to split into four positions. We speculated that this is required to model apical oxygen displacements associated with the supercell. Isotropic thermal parameters were refined independently for O2, O4, and La, while anisotropic thermal ellipsoids were used for the other atoms. The occupancy and the anisotropic thermal parameters of an oxygen atom in the interstitial $8f$ (1/4,1/4,1/4) position (O3) were also refined. This site was previously proposed as the most likely location of the oxygen defect.[19,20] The occupancy of the interstitial site is consistent with an excess oxygen stoichiometry of $\delta \approx 0.09 \pm 0.02$. The refined structural parameters from single-crystal data are listed in Table II.

VIII. RIETVELD REFINEMENT FOR POWDER DATA

The structural parameters of the $\delta \approx 0.08$ and $\delta \approx 0.12$ powder samples, both at room temperature and at 10 K, were refined using the Rietveld technique. All refinements were carried out in the *Fmmm* space group. Initially all atoms were placed in special positions. Refinements that made use of this model led to very large thermal parameters at both temperatures for the O2 atoms. In addition, the occupancy of the O2 position was consistently lower than 2 atoms/f.u.

When thermal parameters for O2 were allowed to be anisotropic, elongated thermal ellipsoids were obtained. The major axis of the ellipsoid was parallel to the [010] direction. This result suggested the existence of static displacements around the high-symmetry position for the O2 atom. Following the scheme already discussed for the single-crystal data, new refinements were attempted with a model that makes use of an additional O4 in a general $h32(x,y,z)$ position, starting in the vicinity of the apical oxygen location. The apical oxygen O2 itself was also allowed to split. The isotropic thermal parameters of O2 and O4 could be refined independently for all data, except the room-temperature data for the $\delta \approx 0.08$ sample, where stability problems were encountered. Since in all other cases the O4 thermal parameter converges to a value close to 1.0, B(O4) was fixed to 1 for this data set. This model converges for all powder data sets, and results in a considerable improvement of the R_{wp} values (typical-

TABLE II. Refined structural parameters from single-crystal neutron diffraction on a $La_2CuO_{4.1}$ sample, at 18 K.

Parameter		Value
$a_t = b_t$[a] (Å)		5.34(2)
c[a] (Å)		13.22(3)
$200 \times (b-a)/(b+a)$[b]		0.8
La	$x = y$	0
	z	0.36054(4)
	n	1.99(2)
	B (Å^2)	0.26(1)
Cu	$x = y = z$	0
	n	1
	u_{11} (Å^2)	0.0002(6)
	u_{22} (Å^2)	0.0036(7)
	u_{33} (Å^2)	0.0069(3)
	$u_{12} = u_{13} = u_{23}$	0
O1	$x = y$	0.25
	z	0
	n	2.10(3)
	u_{11} (Å^2)	0.0065(8)
	u_{22} (Å^2)	0.0046(6)
	u_{33} (Å^2)	0.0155(4)
	u_{12} (Å^2)	−0.0010(2)
	$u_{13} = u_{23}$	0
O2	x	0.0244(6)
	y	0.012(1)
	z	0.1822(1)
	n	1.49(5)
	B (Å^2)	0.25(3)
O3	$x = y = z$	0.25
	n	0.09(3)
	u_{11} (Å^2)	0.02(3)
	u_{22} (Å^2)	0.02(3)
	u_{33} (Å^2)	0.01(1)
	$u_{12} = u_{13} = u_{23}$	0
O4	x	0.016(3)
	y	0.072(4)
	z	0.1797(8)
	n	0.48(8)
	B (Å^2)	0.8(2)
R_{wp}/R_{ex}		2.14

[a]From pseudotetragonal orientation matrix.
[b]From analysis of $[hhl]$ reflections.

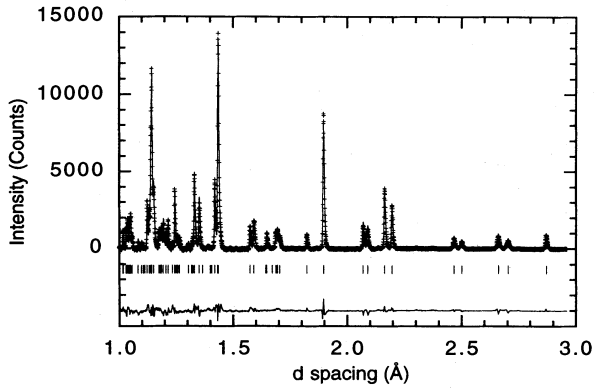

FIG. 8. Rietveld refinement profile for the $La_2CuO_{4.12}$ powder sample at 10 K. The plus (+) signs are the raw time-of-flight neutron powder diffraction data. The solid line is the calculated profile. Tick marks below the diffraction profile mark the position of allowed Bragg reflections. A difference curve (observed minus calculated) is plotted at the bottom.

ly 20%) over the model with O2 in a high-symmetry position. The combined refined occupancies of the O2 and O4 sites is always close to 2, within one standard deviation, without the use of any constraints.

Previous work in the $La_2NiO_{4+\delta}$ system[19] suggested that the O4 atoms were displaced off the high-symmetry position by the presence of the adjacent interstitial oxygen atom. Since the interstitial oxygen site (O3) has four apical oxygen neighbors, one would expect $n(O4) \approx 4 \times n(O3)$. The ratio between the refined value of $n(O4)$ and δ (as obtained from TGA) varies between 3.0 and 4.0 for the various data sets, with an uncertainty of approximately 0.5. We stress the fact that the intensity distribution around the apical oxygen position is averaged over many $\sim 5.4 \times 5.4 \times 13.2$ unit cells that are slightly different, due to the presence of a superstructure. Therefore, any attempt to model this site with a small number of discrete atoms will at best be a good approximation. The large and temperature-independent value of $B(O4)$, for instance, suggests that the displaced apical oxygen itself may form a static displacement wave throughout the supercell.

The occupancy of an oxygen atom in the $8f(1/4,1/4,1/4)$ position was also refined. For powder data, the occupancy converges to a value that is approximately a third of the expected value based on total oxygen content. Attempts to refine O3 in a more general position without damping resulted in divergences. Damped refinements lead back to the $8f$ position within a stan-

TABLE III. Refined structural parameters for powder samples of $La_2CuO_{4.08}$ and $La_2CuO_{4.12}$ at room temperature and 10 K.

		$\delta=0.08$ RT	$\delta=0.08$ 10 K	$\delta=0.12$ RT	$\delta=0.12$ 10 K
a	(Å)	5.35692(4)	5.33353(5)	5.33794(8)	5.32126(7)
b	(Å)	5.38138(5)	5.39489(6)	5.4106(1)	5.40613(8)
c	(Å)	13.1966(1)	13.1561(1)	13.2155(2)	13.1823(2)
V	(Å^3)	380.427(4)	378.551(5)	381.685(7)	379.222(6)
La	$x=y$	0	0	0	0
	z	0.36050(5)	0.36067(6)	0.3601(1)	0.36017(9)
	n	2	2	2	2
	B (Å^2)	0.50(1)	0.27(2)	0.61(3)	0.36(2)
Cu	$x=y=z$	0	0	0	0
	n	1	1	1	1
	B (Å^2)	0.39(2)	0.17(2)	0.45(3)	0.24(3)
O1	$x=y$	0.25	0.25	0.25	0.25
	z	0	0	0	0
	n	2	2	2	2
	B (Å^2)	0.72(2)	0.54(2)	0.70(3)	0.42(3)
O2	x	0.0221(6)	0.013(1)	0	0
	y	0.022(1)	0.0299(6)	0.029(1)	0.0298(9)
	z	0.1820(2)	0.1822(1)	0.1820(2)	0.1817(2)
	n	1.72(4)	1.78(3)	1.69(4)	1.66(4)
	B (Å^2)	0.35(5)	0.20(5)	0.49(6)	0.10(5)
O3	$x=y=z$	0.25	0.25	0.25	0.25
	n	0.010(5)	0.027(6)	0.031(8)	0.036(7)
	B (Å^2)	0.7	0.7	0.7	0.7
O4	x	0.050(3)	0.052(3)	0.046(4)	0.036(4)
	y	0.088(5)	0.109(6)	0.124(6)	0.116(6)
	z	0.191(1)	0.189(2)	0.187(2)	0.188(1)
	n	0.32(4)	0.27(4)	0.36(4)	0.38(5)
	B (Å^2)	1.0	1.0(5)	0.7(6)	1.0(5)
R_{wp}	(%)	5.34	5.86	6.43	6.20
R_{ex}	(%)	3.38	2.99	3.49	2.92

dard deviation. The small amount of interstitial oxygen is inconsistent with the large amount of O2 displaced into the O4 position. However, comparison with the stoichiometric La_2CuO_4 sample demonstrates that the refinement of powder data has poor sensitivity for scattering intensity from the $8f$ position; in fact, attempts to refine the occupancy of the $8f$ position in the stoichiometric sample led to a significant negative value (approximately -0.04), suggesting a systematic error of this magnitude in the refined value of n(O3). If this same systematic error is applied to the electrochemically intercalated samples, the amount of oxygen found in the $(1/4,1/4,1/4)$ position is approximately as expected. A Rietveld refinement profile for the $\delta \approx 0.12$ sample at 10 K is shown in Fig. 8. The structural parameters for the two powder samples at both temperatures are listed in Table III.

IX. DISCUSSION

The lattice parameters of $La_2CuO_{4+\delta}$ for $\delta = 0.00, 0.08$, and 0.12 at 10 and 300 K are plotted in Fig. 9. The in-plane lattice parameters display a pronounced deviation from Vegard's law. In particular, both the average in-plane lattice parameter and the orthorhombic strain are minimum for the 0.08 sample (Fig. 10). This effect, already reported by Grenier and co-workers,[25] can be attributed to the competition between charge doping of the CuO_2 planes and size of the LaO layers. In the stoichiometric La_2CuO_4 material the La-O bond is elongated, with respect to the ideal room-temperature value, by an average of 11.5% along the b axis and by 4.2% along the a axis.[37] The mismatch between the La-O and the Cu-O_2 layers can be quantified by means of the so-called Goldsmidt tolerance factor $t = (\text{La-O})/\sqrt{2}(\text{Cu-O})$.[38] In stoichiometric La_2CuO_4 the room-temperature tolerance factor is significantly lower than 1, indicating that the Cu-O_2 layers are under compression, while the La-O layers are under tension. Therefore, in-plane displacements resulting from the introduction of interstitial oxygen between the La-O layers can be easily accommodated by displacing adjacent oxygen atoms. Refinements of the displaced apical oxygen position confirm that these displacements occur preferentially in the b direction. The behavior of the in-plane lattice parameters at low interstitial oxygen concentration is therefore dominated by the in-plane Cu-O bond length, that is expected to decrease almost linearly as a function of added charge, as it does in the $La_{2-x}Sr_xCuO_4$ system.[39] At higher defect concentration, the tolerance factor will approach and ultimately exceed 1, leading to an increase of the average in-plane lattice parameter [Fig. 10(a)]. A phase transition between the *Bmab* and the *Fmmm* + superstructure phases occurs between the two regimes. Interstitial oxygen ordering is the most likely explanation for the increased orthorhombicity [Fig. 10(b)].

The c lattice parameter increases continuously with in-

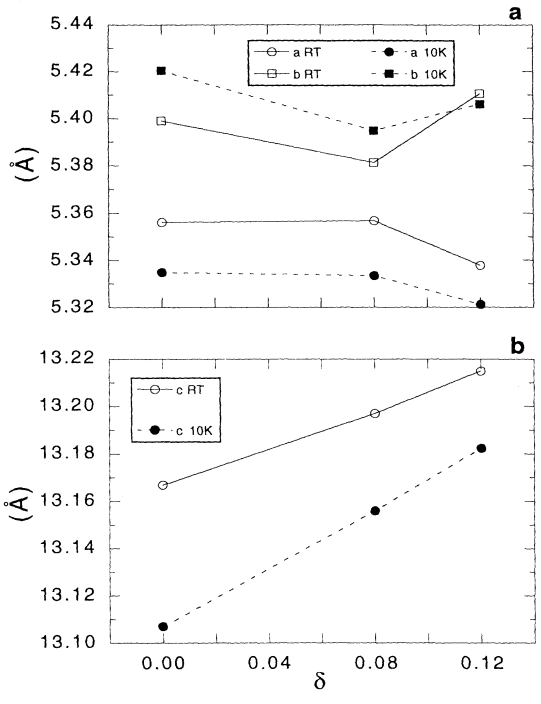

FIG. 9. In-plane lattice parameters (a) and c lattice parameter (b) as a function of excess oxygen content δ, from neutron powder diffraction data. Open and filled symbols indicate values at room temperature and at 10 K, respectively. Error bars from Rietveld refinements are smaller than the symbols.

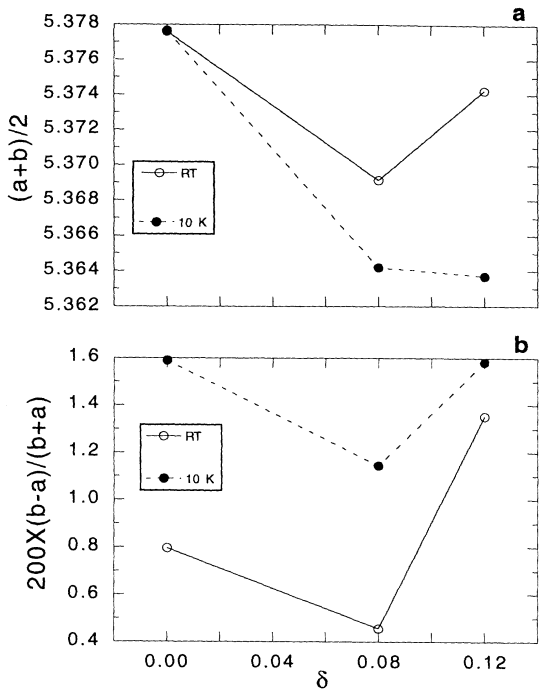

FIG. 10. Average in-plane lattice parameter $(a+b)/2$ (a) and orthorhombic strain $200\times(b-a)/(b+a)$ (b), as a function of excess oxygen content δ, from neutron powder diffraction data. Open and filled symbols indicate values at room temperature and at 10 K, respectively. Error bars from Rietveld refinements are smaller than the symbols.

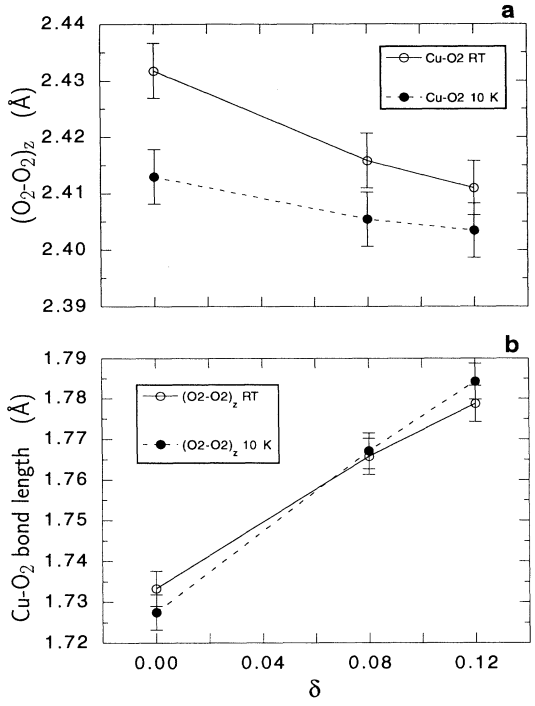

FIG. 11. Cu-O2 bond length (a) and z component of the O2-O2 vector (b), as a function of excess oxygen content δ, from neutron powder diffraction data. Open and filled symbols indicate values at room temperature and at 10 K, respectively. Error bars from Rietveld refinements are indicated.

creasing oxygen content. This elongation is the net result of an expansion of the LaO interlayer distance in the z direction, consistent with the introduction of interstitial oxygen between the LaO layers, and a comparatively smaller contraction of the Cu-O2 distance (Fig. 11). Reductions of the copper-apical oxygen distance are commonly observed in superconducting cuprates as a consequence of charge doping of the CuO_2 layers. In the present case, this reduction is smaller than the simultaneous increase in the La_2O_2 layer thickness.

The defect structure arising from the introduction of interstitial oxygen atoms is manifestly very complicated. A clear picture can emerge only by solving the superstructure. The solution of the average structure, however, provides some constraints on the possible ordering modes of the superstructure. First, it is clear that the atomic displacements from high-symmetry positions are not ordered at the level of the fundamental $\sim 5.4 \times 5.4 \times 13.2$ Å^3 unit cell. The magnitude of the O2 displacement from the (0,0,z) position in either oxygen-rich sample is comparable to the displacement resulting from tilting in the stoichiometric material. Therefore, any ordering of such displacements at the level of a fundamental unit cell would result in low-symmetry peaks of comparable intensity. The existence of a large superstructure suggests that the ordering patterns of the interstitial oxygen atoms and of the apical oxygen displacements span many fundamental unit cells. A likely hypothesis is that the O2 atoms order in such a way as to create a number of enlarged tetrahedral holes for the O3 atoms, with apical oxygen atoms adjacent to the occupied holes being further displaced into the O4 positions. An alternative explanation is that ordering creates a network of short O—O distances between apical and interstitial oxygen atoms. The possibility of a short O—O bond has already been discussed by Chaillout and co-workers,[21] in the context of the *Bmab* space group. According to our interpretation of the crystallographic data, the ordering of the short bonds would occur in a large supercell. A short O—O bond will necessarily have a strong covalent character, which would be consistent with the observed discrepancy between TGA and iodometric titration data.

ACKNOWLEDGMENTS

This work was supported by the NSF Office of Science and Technology Centers under Contract No. DMR 91-20000 (PGR,BAH,JLW), by the U.S. Department of Energy, Basic Energy Sciences-Materials Sciences, under Contract W-31-109-ENG-38 (JDJ, AJS). Ames laboratory is operated for the U.S. Department of Energy by Iowa State University under Contract No. W-7405-ENG-82. The work at Ames (FCC,DCJ) was supported by the Office of Basic Energy Sciences. We wish to thank S.-W. Cheong for kindly providing us with a La_2CuO_4 single crystal, and Gian Felcher and Hagai Shaked for their contribution of ideas and discussions.

[1]J. B. Torrance, A. Bezinge, A. I. Nazzal, T. C. Huang, S. S. Parkin, D. T. Keane, S. J. LaPlaca, P. N. Horn, and G. A. Held, Phys. Rev. B **40**, 8872 (1989).

[2]J. D. Axe, A. H. Moudden, D. Hohlwein, D. E. Cox, K. M. Mohanty, A. R. Moodenbaugh, and Y. Xu, Phys. Rev. Lett. **62**, 2751 (1989).

[3]K. Oh-Ishi and Y. Syono, J. Solid State Chem. **95**, 136 (1991).

[4]C. C. Torardi, M. A. Subramanian, J. Gopalakrishnan, and A. W. Sleight, Physica C **158**, 465 (1989).

[5]J. Beille, R. Cabanel, C. Chaillout, B. Chevalier, G. Demazeau, F. Deslandes, J. Etoutneau, P. Lejay, C. Michel, J. Provost, B. Raveau, A. Sulpice, J. L. Tholence, and R. Tournier, C.R. Acad. Sci. Ser. B **304**, 1097 (1987).

[6]P. M. Grant, S. S. P. Parkin, V. Y. Lee, E. M. Engler, M. L. Ramirez, J. E. Vazquez, G. Lim, and R. D. Jacowitz, Phys. Rev. Lett. **58**, 2482 (1987).

[7]K. Sekizawa, Y. Takano, H. Takigami, S. Tasaki, and T. Inaba, Jpn. J. Appl. Phys. **26**, L840 (1987).

[8]J. E. Schirber, E. L. Venturini, B. Morosin, J. F. Kwak, D. S. Ginley, and R. J. Baughman, in *High-temperature Superconductors,* edited by M. B. Brodsky (Materials Research Society, Pittsburgh, 1988), p. 479.

[9]G. Demazeau, F. Tresse, T. Plante, B. Chevalier, J. Etourneau, C. Michel, M. Hervieu, B. Raveau, P. Lejay, A. Sulpice, and R. Tournier, Physica C **153-155**, 824 (1988).

[10]J. Zhou, S. Sinha, and J. B. Goodenough, Phys. Rev. B **39**, 12 331 (1989).

[11]J. D. Jorgensen, B. Dabrowski, D. G. Hinks, S. Pei, H. B.

Vanfleet, and D. L. Decker (unpublished).
[12]J. E. Schirber, B. Morosin, R. M. Merrill, P. F. Hlava, E. L. Venturini, J. F. Kwak, P. J. Nigrey, R. J. Baughman, and D. S. Ginley, Physica C **152**, 121 (1988).
[13]J. W. Rogers, Jr., N. D. Shinn, J. E. Schirber, E. L. Venturini, D. S. Ginley, and B. Morosin, Phys. Rev. B **38**, 5021 (1988).
[14]B. Andraka, U. Ahlheim, J. S. Kim, G. Fraunberger, G. R. Stewart, B. Morosin, E. L. Venturini, D. S. Ginley, and J. E. Shirber, Phys. Rev. B **42**, 10016 (1990).
[15]J. D. Jorgensen, B. Dabrowski, S. Pei, D. G. Hinks, L. Soderholm, B. Morosin, J. E. Schirber, E. L. Venturini, and D. S. Ginley, Phys. Rev. B **38**, 11 337 (1988).
[16]B. Dabrowski, D. G. Hinks, J. D. Jorgensen, and D. R. Richards, *High-Temperature Superconductors: Relationship Between Properties, Structure and Solid State Chemistry* (Materials Research Society, Pittsburgh, 1989), p. 69.
[17]B. Dabrowski, J. D. Jorgensen, D. G. Hinks, S. Pei, D. R. Richards, H. B. Vanfleet, and D. L. Decker, Physica C **162-164**, 99 (1989).
[18]D. J. Buttrey, P. Ganguly, J. M. Honig, C. N. R. Rao, R. R. Schartman, and G. N. Subbanna, J. Solid State Chem. **74**, 233 (1988).
[19]J. D. Jorgensen, B. Dabrowski, S. Pei, D. R. Richards, and D. G. Hinks, Phys. Rev. B **40**, 2187 (1989).
[20]C. Chaillout, S.-W. Cheong, Z. Fisk, M. S. Lehmann, M. Marezio, B. Morosin, and J. E. Schirber, Physica C **158**, 183 (1989).
[21]C. Chaillout, J. Chenavas, S.-W. Cheong, Z. Fisk, M. Marezio, and B. Morosin, Phsyica C **170**, 87 (1990).
[22]P. Rudolf and R. Schöllhorn, J. Chem. Soc. D 1158 (1992).
[23]A. Wattiaux, J. C. Park, J.-C. Grenier, and M. Pouchard, C. R. Acad. Sci. Ser. B **310**, 1047 (1990).
[24]J.-C. Grenier, A. Wattiaux, and M. Pouchard (unpublished).
[25]J.-C. Grenier, N. Lagueyte, A. Wattiaux, J.-P. Doumerc, P. Dordor, J. Etourneau, M. Pouchard, J. B. Goodenough, and J. S. Zhou, Physica C **202**, 209 (1992).
[26]F. C. Chou, J. H. Cho, and D. C. Johnston, Physica C **197**, 303 (1992).
[27]S.-W. Cheong, Z. Fisk, J. O. Willis, S. E. Brown, J. D. Thompson, J. P. Remeika, A. S. Cooper, R. M. Aikin, D. Schiferl, and G. Gruner, Solid State Commum. **65**, 111 (1988).
[28]D. C. Johnston, J. Magn. Magn. Mater. **100**, 218 (1991).
[29]J. D. Jorgensen, J. Faber, Jr., J. M. Carpenter, R. K. Crawford, J. R. Haumann, R. L. Hitterman, R. Kleb, G. E. Ostrowski, F. J. Rotella, and T. G. Worlton, J. Appl. Crystallogr. **22**, 321 (1989).
[30]R. B. von Dreele, J. D. Jorgensen, and C. J. Windsor, J. Appl. Crystallogr. **15**, 581 (1982).
[31]F. J. Rotella, *User Manual for Rietveld Analysis of Time-of-Flight Neutron Powder Diffraction Data at IPNS* (ANL, Argonne, IL, 1988).
[32]A. J. Schultz, Trans. Am. Crystallogr. Assoc. **23**, 61 (1987).
[33]A. J. Schultz, J. Phys. (Paris) Colloq. **47**, C5 (1986).
[34]W. R. Busing, K. O. Martin, and H. A. Levy, ORFLS (ORNL, Oak Ridge, TN, 1962).
[35]Z. Hiroi, T. Obata, M. Takano, and Y. Bando, Phys. Rev. B **41**, 11 665 (1990).
[36]A. Demourgues, F. Weill, B. Darriet, A. Wattiaux, J. C. Grenier, P. Gravereau, and M. Pouchard (unpublished).
[37]R. D. Shannon, Acta Crystallogr. A **32**, 751 (1976).
[38]J. B. Goodenough and A. Manthiram, J. Solid State Chem. **88**, 115 (1990).
[39]D. G. Hinks, J. D. Jorgensen, A. W. Mitchell, B. A. Hunter, B. Dabrowski, J. L. Wagner, and P. G. Radaelli (unpublished).